CHEMICAL ENGINEERING TRANSACTIONS
VOL. 79, 2020
A publication of AIDIC
The Italian Association of Chemical Engineering
Online at www.cetjournal.it
Guest Editors: Enrico Bardone, Antonio Marzocchella, Marco Bravi

ISBN 978-88-95608-77-8; **ISSN** 2283-9216
DOI: 10.3303/CET2079072

Fe_3O_4/Graphene Electrode for the ELectrochemical Detection of 4-Ntrophenol

Maria Sarno[a,b]*, Eleonora Ponticorvo[b]

[a] Department of Physics "E.R. Caianiello", University of Salerno, Via Giovanni Paolo II, 132, 84084, Fisciano (SA), Italy.
[b] NanoMates, Research Centre for Nanomaterials and Nanotechnology at the University of Salerno, University of Salerno, Via Giovanni Paolo II, 132, 84084, Fisciano (SA), Italy.
msarno@unisa.it

Here the performance in 4-Nitrophenol (4-NP) detection of magnetite-few layer graphene-based electrode was reported. The prepared nanocomposite, synthesized according to a "wet chemistry" approach, was broadly characterized: SEM and TEM images and XRD spectra indicate the formation of nanoparticles with a few nanometers size dispersed on graphene layers. The sample was tested as an electrochemical sensor for the detection of small traces of 4-NP in aqueous solutions with a limit of detection (LOD) of 4 μM. The sensor was tested also for 1 month, showing proper operation and excellent stability.

1. Introduction

Phenol compounds are important intermediates in drugs, dyestuffs and pesticides synthesis (Yu et al., 2019). These compounds have a remarkable role in agriculture due to high insecticidal activity, but, at the same time, even at very low concentrations, lead to irreversible damage to organisms and plants (Saleem et al., 2018). Among these, 4-Nitrophenol (4-NP), a chemical intermediate in the production of organophosphorus insecticidal derivatives, is considered a key pollutant by the United States Environmental Protection Agency; therefore, growing interest in developing methods for determining and the removal of this compound has been raised. Several techniques (e.g. capillary zone electrophoresis, UV-vis spectrophotometry, fluorescence, gas and liquid chromatography) have been studied for the determination of 4-NP. However, to implement these approaches, expensive devices and long analysis time are required.
Electrochemical techniques have drawn increasing attention thanks to the intrinsic advantages of these methods (i.e. simplicity, easy operation, short analysis time, high sensitivity, the capability of on-line monitoring and low cost) (Sarno et al., 2019a; Rahman et al., 2018). Electrochemical sensors were applied to detect a variety of materials, such as heavy metals, DNA hybridization, polycyclic aromatic hydrocarbons, polychlorinated biphenyls, pesticides, glucose and so on (Yogeswaran and Chen, 2008; Thiyagarajan et al., 2014; Sarno and Ponticorvo, 2019a; Sarno and Ponticorvo, 2019b).
Graphene, a two-dimensional structure consisting of sp_2-hybridized carbon, attracted significant attention because of its chemical stability, high specific surface area, outstanding charge transport mobility, mechanical strength and so on. Graphene-based materials were applied for new energy batteries, flexible screens, supercapacitors**,** and innovative sensors (Sarno et al., 2016; Ambrosi et al., 2016; Ciambelli et al., 2004). On the other hand, the extensive research work has been done related to magnetite (Fe_3O_4) (Setyawan and Widiyastuti, 2019; Ali et al., 2016; Sarno et al., 2019b) nanoparticles due to their special qualities, such as low cost, easy preparation, low toxicity, magnetic and optical properties, and biocompatibility (Gerent and Spinelli, 2017; Bharath et al., 2015). Hybrid structures, constituted by two or more nanomaterials, have shown some interesting catalytic properties thanks to the interfacial interactions between different components. This is seen in enhanced catalytic power, obtaining nanostructures more active than either single material. Herein, a novel 4-nitrophenol sensor with superior electrocatalytic performance, obtained by modifying the glassy carbon electrode with a synthesized Fe_3O_4-graphene nanohybrid, was reported. The electrocatalytic performance sensor was evaluated by cyclic voltammogram (CV) and differential pulse voltammetry (DPV) analysis. The proposed sensor exhibits low detection limit**s** and high sensitivity. Scanning Electron Microscopy (SEM),

Paper Received: 12 September 2019; Revised: 20 January 2020; Accepted: 26 February 2020
Please cite this article as: Sarno M., Ponticorvo E., 2020, Fe3o4/graphene Electrode for the Electrochemical Detection of 4-nitrophenol, Chemical Engineering Transactions, 79, 427-432 DOI:10.3303/CET2079072

Transmission Electron Microscopy–Energy-dispersive X-ray spectroscopy (TEM-EDS) and X-ray diffraction (XRD) were employed for materials characterization.

2. Experimental Section

2.1 Nanocomposite preparation

Few-Layer Graphene (in the following "G") was obtained by sonication of graphite in N-methylpyrrolidone (NMP, spectrophotometric grade> 99.0%) (Guadagno et al., 2015; Sarno et al., 2015). After subsequent centrifugations, G: with a lateral sizes of few micrometers; a number fraction of monolayer graphene (number of monolayers/total number of flakes) equal to 22%; more than 85% of the number of the total sheet have layers ranging from 1 to 6; and a fraction of the total sheets with layers raging between 25-40, was recovered.
Fe_3O_4 dispersed on G based nanocomposite, in the following named Fe_3O_4/G, was obtained using standard airless procedures and commercially available reagents. Fe_3O_4/G was prepared by thermal decomposition of iron acetylacetonate in an organic solvent in the presence of G with a Fe_3O_4/G weight ratio equal to 0.15, using oleic acid and oleylamine as surfactant agents (Liu et al., 2015; Tripathy and Mishra, 2017).

2.2 Characterization methods

A Bruker D8 X-ray diffractometer with monochromatic CuKα radiation was used for measurements of powder diffraction profiles. TEM images were acquired using FEI Tecnai electron microscope, operating at 200 kV with a LaB_6 filament as the source of electrons, equipped with an energy-dispersive X-ray spectroscopy (EDX) probe. For the preparation of the TEM sample, 0.1 mg of the nanocomposite dispersed in hexane was deposited on carbon-coated electron microscope grids. Scanning electron microscopy (SEM) images were obtained by the use of a Phenom electron microscope, equipped with an energy dispersive X-ray (EDX) probe.
Electrochemical characterization was carried out by means of Autolab PGSTAT302N potentiostat/galvanostat. In detail, a conventional three-electrode system was composed of a glassy carbon electrode (GCE) as the working electrode, a Pt foil as the counter electrode, and Ag/AgCl (3 M KCl saturated with AgCl) as the reference electrode, respectively. Cyclic voltammogram (CV) and differential pulse voltammetry (DPV) tests were performed in a wide 4-nitrophenol concentration range (10-500 μM).

3. Results and discussion

The XRD spectrum of the prepared nanocomposite is shown in Figure 1.

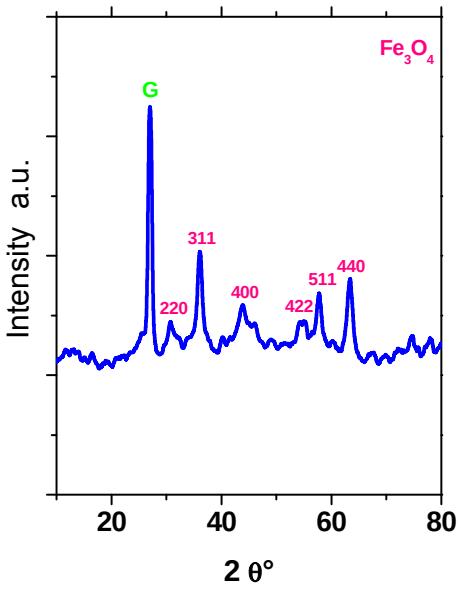

Figure 1: XRD spectrum of Fe_3O_4/G.

A series of characteristic peaks: (220), (311), (400), (4 2 2), (511), and (440), which are in good agreement with the inverse cubic spinel phase of Fe_3O_4 (magnetite, JCPDS card no. 85-1436), were observed. These results are similar to those reported in the literature (Wang et al., 2011; Yang et al., 2018). The mean crystallite diameter obtained from the diffractogram, by using the Scherrer's formula, is 7 nm. Furthermore, the typical peak at (002) of pristine graphite is visible, which intensity is comparable with that of nanoparticles indicating delamination of the graphite into more thinner graphene and multilayer graphene sheets (Sarno et al., 2012).

To evaluate the morphology of the as-prepared nanocomposite, a TEM image is shown in Figure 2a. The image revealed that the Fe_3O_4 NPs, with uniform size, are attached to the G sheets even after the ultrasonication used to disperse Fe_3O_4/G for TEM characterization. The particle size distribution, obtained from the statistical analysis of over 100 NPs showed that the average diameter of the inorganic core is d = 7.2 nm with σ = 1.05 nm. The corresponding electron diffraction pattern, not shown here, confirms the ferrite nature of nanocrystals.

SEM image of Fe_3O_4/G was reported in Figure 2b. The EDX maps provided information about the nanoparticle's disposition both topographically and quantitatively. Iron and oxygen were homogeneously distributed on carbon, their maps, superimposable to this of carbon, were also given in Figure 2b.

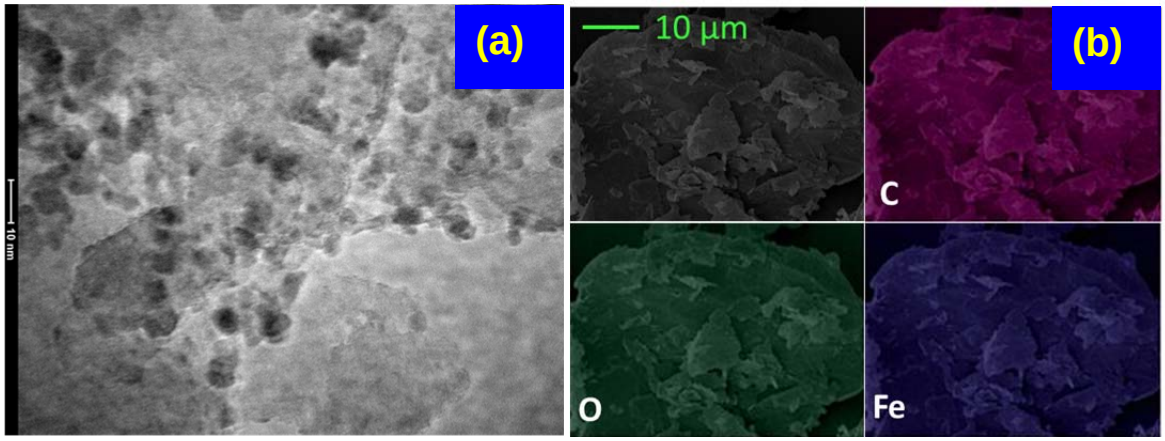

Figure 2: TEM image of Fe_3O_4/G (a) and SEM image of Fe_3O_4/G and EDX maps of carbon, oxygen, and iron (b).

The N_2 adsorption-desorption isotherm of prepared nanocomposites is shown in Figure 3. A BET surface area of 512 m^2/g due to the G content and a mesoporosity between G sheets (total pore volume 1.10 cm^3/g, micropore volume 0.16 cm^3/g), were observed.

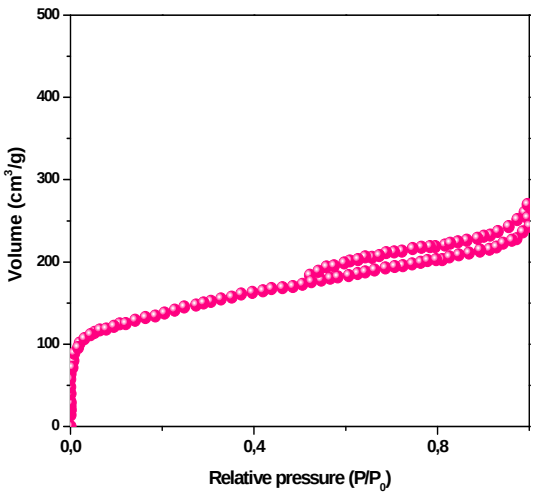

Figure 3: Nitrogen adsorption-desorption isotherms of Fe_3O_4/G.

The multimodal mesopore size distribution (BJH (Barrett-Joyner-Halenda) pore distribution) is centered at 2.7 (interparticle surface porosity), 16 and 35 nm (pores between nanoparticles aggregates). A microporosity ensuring a suitable surface area was observed together with mesopores (Villarroel-Rocha et al., 2014).
4-NP was detected by CV and DPV measurements on the Fe_3O_4/G nanocomposite deposited on a GCE electrode over the very wide concentration range of 10-500 µM. In Figure 4, the DPV curves obtained at different concentrations of 4-NP over the concentration range of 100-500 µM, are shown. The potential peak for electrochemical 4-NP detection is observed at ~ 1 V.

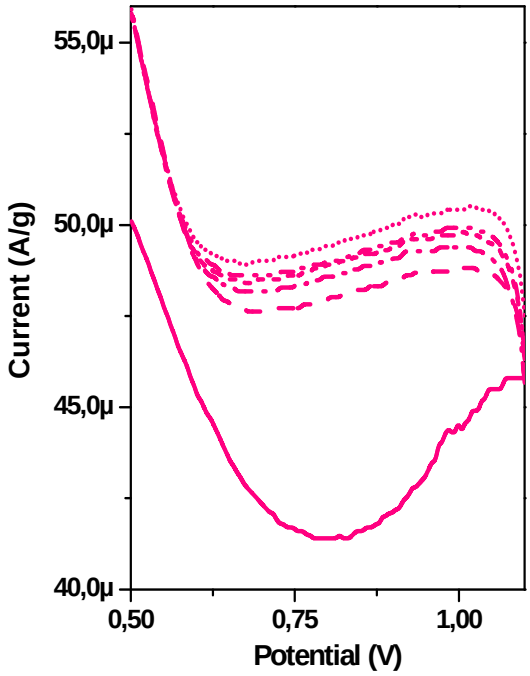

Figure 4: DPV curves of Fe_3O_4/G for various 4-NP concentrations. The continuous line indicates the results obtained with a solution without 4-NP. Amplitude: 25mV; Scan rate: 10 mV s^{-1}.

In Figure 5a the linear relationship between the peak currents and the concentrations from 0.01 mM to 0.10 mM can be observed. The linear equation (R^2 of 0.969) is:

I (µA) = *4.04*10^-5+8.067*10^-5*C (mM)* (1)

where C is the 4-NP concentration.
The limit of detection (LOD) and the limit of quantification (LOQ) were calculated using the following equations:

$$LOD = \frac{3*\delta}{b} \quad (2)$$

$$LOQ = \frac{10*\delta}{b} \quad (3)$$

where δ is the standard deviation, b is the slope of the calibration curve (Sarno et al., 2019a).
The calculated LOD and LOQ are 0.004 mM and 0.016 mM, respectively.
In order to determine the storage stability of the Fe_3O_4/G electrode, its 4-NP detection performance was monitored for 1 month. Figure 5b shows the relationship between the peak current at different days. During 30 days storage period, the electrode retained 97% of the initial response current, revealing good storage stability, higher than that reported in the literature so far (Tang et al., 2013).

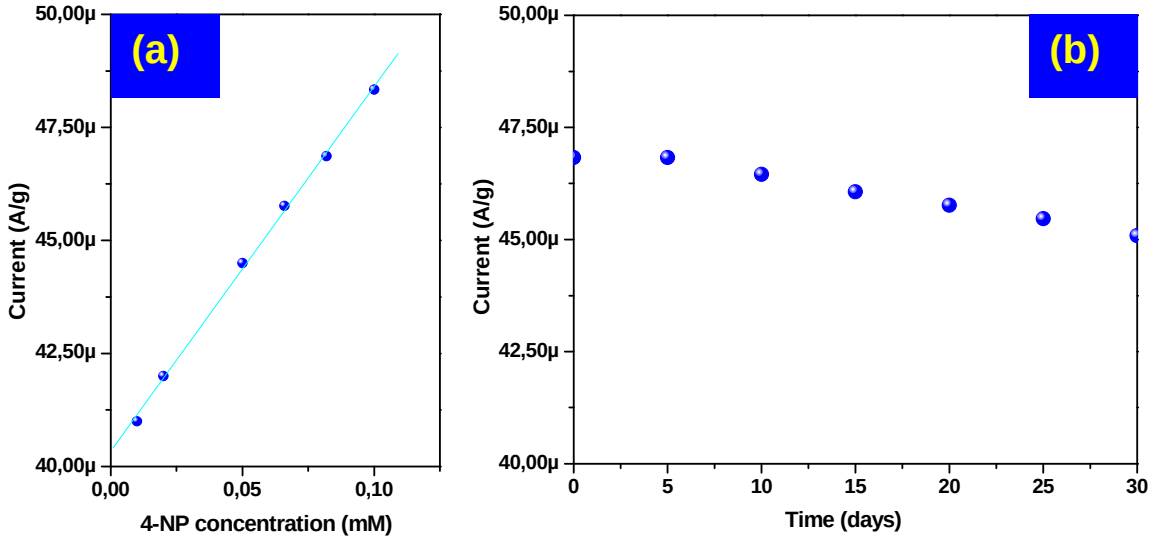

Figure 5: Calibration plot of the DPV curves in the 4-NP concentration range 0.01-0.1mM (a). Peak current of different storage days of 4-NP by DPV response. Amplitude: 25mV; Scan rate: 10 mV s^{-1} (b).

The Fe_3O_4/G electrode was further explored to detect the 4-NP in tap water for the real sample analysis. The accuracy of the detection of 4-NP was obtained through DPV in real samples. The obtained results are summarized in Table 1, confirming the good electrochemical responses. The obtained recovery values range from 96% and 100%, which reveals the appreciable practicality of the 4-NP sensor.

Table 1: Determination of 4-NP in tap water samples using DPV analysis

4-NP added [mM]	4-NP detected [mM]	Recovery [%]
0.01	0.01	100
0.05	0.049	98
1	0.957	96
10	9.540	96
100	98.82	99

4. Conclusions

In summary, a simple and efficient strategy was applied to synthesize magnetite nanoparticles dispersed on few-layer graphene. TEM and SEM images confirmed the formation of the aforementioned nanocomposite structure. The prepared nanocomposite has been tested as an electrochemical sensor in order to detect small traces of 4-NP in aqueous solutions.

Fe_3O_4/G electrode showed excellent behavior as 4-NP sensor: high peak currents intensities, excellent linear ranges of detection (10-500 µM), low detection limit (0.004 mM) and favorable stability. So this sensor may be a good and cheap choice in practical applications.

References

Ali A., Zafar H., Zia M., ul Haq I., Phull A.R., Ali J.S., Hussain A., 2016, Synthesis, characterization, applications, and challenges of iron oxide nanoparticles, Nanotechnology, Science and Applications, 9, 49-67.

Ambrosi A., Chua C.K., Latiff N.M., Loo A.H., Wong C.H.A., Eng A.Y.S., Bonanni A., Pumera M., 2016, Graphene and its electrochemistry – an update, Chemical Society Reviews, 45, 2458-2493.

Bharath G., Veeramani V., Chen S.-M., Madhu R., Raja M.M., Balamurugan A., Mangalaraj D., Viswanathana C., Ponpandian N., 2015, Edge-carboxylated graphene anchoring magnetite-hydroxyapatite nanocomposite for an efficient 4-nitrophenol sensor, RSC Advances, 5, 13392-13401.

Ciambelli P., Sannino D., Sarno M., Fonseca A., Nagy J.B., 2004, Hydrocarbon decomposition in alumina membrane: an effective way to produce carbon nanotubes bundles, Journal of Nanoscience and Nanotechnology, 4, 779-787.

Gerent G.G., Spinelli A., 2017, Magnetite-platinum nanoparticles-modified glassy carbon electrodeas electrochemical detector for nitrophenol isomers, Journal of Hazardous Materials, 330,105-115.

Guadagno L., Sarno M., Vietri U., Raimondo M., Cirillo C., Ciambelli P., 2015, Graphene-based structural adhesive to enhance adhesion performance, RSC Advances, 5, 27874-27886.

Liu S., Guo S., Sun S., You X.Z., 2015, Dumbbell-like Au-Fe_3O_4 nanoparticles: a new nanostructure for supercapacitors, Nanoscale, 7, 4890-4893.

Rahman M.M., Alam M.M., Asiri A.M., 2018, 2-Nitrophenol sensor-based wet-chemically prepared binary doped Co_3O_4/Al_2O_3 nanosheets by an electrochemical approach, RSC Advances, 8, 960-970.

Saleem H., Rehman K., Arslan M., Afzal M., 2018, Enhanced degradation of phenol in floating treatment wetlands by plant-bacterial synergism, International Journal of Phytoremediation, 20, 692-698.

Sarno M., Cirillo C., Ponticorvo E., Ciambelli P., 2015, Synthesis and Characterization of FLG/Fe_3O_4 Nanohybrid Supercapacitor, Chemical Engineering Transactions, 43, 727-732.

Sarno M., Cirillo C., Scudieri C., Polichetti M., Ciambelli P., 2016, Electrochemical Applications of Magnetic Core–Shell Graphene-Coated FeCo Nanoparticles, Industrial and Engineering Chemistry Research, 55, 3157-3166.

Sarno M., Ponticorvo E., 2019a, Metal–metal oxide nanostructure supported on graphene oxide as a multifunctional electro-catalyst for simultaneous detection of hydrazine and hydroxylamine, Electrochemistry Communications, 107, 106510.

Sarno M., Ponticorvo E., Scarpa D., 2019a, Controlled PtIr nanoalloy as an electro-oxidation platform for methanol reaction and ammonia detection, Nanotechnology, 30, 394004.

Sarno M., Sannino D., Leone C., Ciambelli P., 2012, Evaluating the effects of operating conditions on the quantity, quality and catalyzed growth mechanisms of CNTs, Journal of Molecular Catalysis A: Chemical, 357, 26-38.

Sarno M., Scudieri C., Ponticorvo E., 2019b, Flower-like AuPtPd-Fe_3O_4 Nanocatalyst for Electrochemical Removal of Humic Acids and Cr(VI), Chemical Engineering Transactions, 73, 229-234.

Sarno M., Ponticorvo E., 2019b, High hydrogen production rate on RuS_2@MoS_2 hybrid nanocatalyst by PEM electrolysis, International Journal of Hydrogen Energy 44, 4398-4405.

Setyawan H., Widiyastuti W., 2019, Progress in the Preparation of Magnetite Nanoparticles through the Electrochemical Method, KONA Powder and Particle Journal, 36, 145-155.

Tang Y., Huang R., Liu C., Yang S., Lu Z., Luo S., 2013, Electrochemical detection of 4-nitrophenol based on a glassy carbon electrode modified with a reduced graphene oxide/Au nanoparticle composite, Analytical Methods, 5, 5508-5514.

Thiyagarajan N., Chang J.-L., Senthilkumar K., Zen J.-M., 2014, Disposable electrochemical sensors: a mini review, Electrochemistry Communications, 38, 86-90.

Tripathy D.B., Mishra A., 2017, Convenient synthesis, characterization and surface active properties of novel cationic gemini surfactants with carbonate linkage based on C_{12}-C_{18} sat./unsat. fatty acids, Journal of Applied Research and Technology, 15, 93-101.

Villarroel-Rocha J., Barrera D., Sapag K., 2014, Introducing a self-consistent test and the corresponding modification in the Barrett, Joyner and Halenda method for pore-size determination, Microporous and Mesoporous Materials, 200, 68-78.

Wang Y.M., Cao X., Liu G.H., Hong R.Y., Chen Y.M., Chen X.F., Li H.Z., Xu B., Wei D.G., 2011, Synthesis of Fe_3O_4 magnetic fluid used for magnetic resonance imaging and hyperthermia, Journal of Magnetism and Magnetic Materials, 323, 2953-2959.

Yang L., Tian J., Meng J., Zhao R., Li C., Ma J., Jin T., 2018, Modification and Characterization of Fe_3O_4 Nanoparticles for Use in Adsorption of Alkaloids, Molecules, 23, 562.

Yogeswaran U., Chen S.-M., 2008, A Review on the Electrochemical Sensors and Biosensors Composed of Nanowires as Sensing Material, Sensors, 8, 290-313.

Yu Z.-H., Gan Y.-L., Xu J., Xue B., 2019, Direct Catalytic Hydroxylation of Benzene to Phenol Catalyzed by $FeCl_3$ Supported on Exfoliated Graphitic Carbon Nitride, Catalysis Letters, 1-11.